Metabolic Engineering 14 (2012) 47–58

Contents lists available at SciVerse ScienceDirect

Metabolic Engineering

journal homepage: www.elsevier.com/locate/ymben

Integration of *in vivo* and *in silico* metabolic fluxes for improvement of recombinant protein production

Habib Driouch, Guido Melzer, Christoph Wittmann*

Institute of Biochemical Engineering, Technische Universität Braunschweig, Gaussstraße 17, 38106 Braunschweig, Germany

ARTICLE INFO

Article history:
Received 28 March 2011
Received in revised form
12 October 2011
Accepted 2 November 2011
Available online 20 November 2011

Keywords:
Fructofuranosidase
Aspergillus niger
^{13}C metabolic flux
Metabolic engineering
Filamentous fungi
Elementary mode

ABSTRACT

The filamentous fungus *Aspergillus niger* is an efficient host for the recombinant production of the glycosylated enzyme fructofuranosidase, a biocatalyst of commercial interest for the synthesis of prebiotic sugars. In batch culture on a minimal glucose medium, the recombinant strain *A. niger* SKAn1015, expressing the fructofuranosidase encoding *suc1* gene secreted 45 U/mL of the target enzyme, whereas the parent wild type SKANip8 did not exhibit production. The production of the recombinant enzyme induced a significant change of *in vivo* fluxes in central carbon metabolism, as assessed by ^{13}C metabolic flux ratio analysis. Most notably, the flux redistribution enabled an elevated supply of NADPH via activation of the cytosolic pentose phosphate pathway (PPP) and mitochondrial malic enzyme, whereas the flux through energy generating TCA cycle was reduced. In addition, the overall possible flux space of fructofuranosidase producing *A. niger* was investigated *in silico* by elementary flux mode analysis. This provided theoretical flux distributions for multiple scenarios with differing production capacities. Subsequently, the measured flux changes linked to improved production performance were projected into the *in silico* flux space. This provided a quantitative evaluation of the achieved optimization and a priority ranked target list for further strain engineering. Interestingly, the metabolism was shifted largely towards the optimum flux pattern by sole expression of the recombinant enzyme, which seems an inherent attractive property of *A. niger*. Selected fluxes, however, changed contrary to the predicted optimum and thus revealed novel targets—including reactions linked to NADPH metabolism and gluconate formation.

© 2011 Elsevier Inc. All rights reserved.

1. Introduction

Aspergillus niger is an attractive industrial producer of organic acids as well as various extracellular enzymes and antibiotics (Hofmann et al., 2009). As eukaryotic organism, *A. niger* offers valuable advantages for enzyme secretion such as facilitated proteolytic processing and protein folding as well as posttranslational modifications (Lubertozzi and Keasling, 2009; Nevalainen et al., 2005). Towards understanding of its cellular metabolism and superior production it is probably the filamentous fungus, which receives the greatest interest with respect to its metabolic capabilities (Andersen et al., 2008; de Jongh and Nielsen, 2008; Panagiotou et al., 2009a,b). One of the recently emerging enzymes available through recombinant *A. niger* strains is fructofuranosidase (EC 3.2.1.26), an important biocatalyst for the synthesis of rare neo-sugars as functional food ingredients (Maiorano et al., 2008). In particular, these compounds are attractive for human consumption, since they reduce the risk of colon cancer (Pool-Zobel et al., 2002). The creation of an *A. niger* strain with high expression of the recombinant product encoding gene (Fleissner and Dersch, 2010), medium design and bioprocess optimization have recently enabled an efficient production process for fructofuranosidase (Driouch et al., 2010a,b; Driouch et al., 2011b). With minimal pre-treatment of the secreted enzyme, this allows the biosynthesis of 450 g/L of neo-sugars of the inulin type, prebiotics with substantial commercial interest, within short time (Driouch et al., 2011a). This promising situation now drives increasing interest on the underlying metabolism of *A. niger* towards further optimization. Hereby, metabolic flux analysis seems most useful to unravel metabolic engineering targets due to the close correlation of the metabolic fluxes to the cellular phenotype. Concerning *A. niger*, metabolic flux analysis, which evolved from pioneering studies on small stoichiometric models (Pedersen et al., 2000; Schmidt et al., 1999) has revealed a high flexibility of the metabolism *A. niger* in response to the nutrient status, the genetic background or the type of product formed (Andersen et al. 2008; Meijer et al. 2009). Beyond experimental flux studies, *in silico* pathway analysis has enabled a detailed view into the theoretical flux space of *A. niger* for various scenarios (Andersen et al., 2008; Melzer et al., 2009). These are attractive from their straightforward strategy to directly exploit stoichiometric network information and allow broad simulation studies on various aspects (Kim et al., 2008).

The present work integrates physiological flux information from strains under investigation into strain design—by combining the power of the computational network simulation with the resolution

* Corresponding author: Fax: +49 531 391 7652.
E-mail address: c.wittmann@tu-bs.de (C. Wittmann).

1096-7176/$ - see front matter © 2011 Elsevier Inc. All rights reserved.
doi:10.1016/j.ymben.2011.11.002

of experimental network analysis on the flux level. Particularly, it integrates *in vivo* with *in silico* flux data to investigate the impact of recombinant protein production on central carbon metabolism. For this purpose intracellular fluxes were compared between a fructofuranosidase producing recombinant strain of *A. niger* and its parent wild type. A compartmented large-scale metabolic model of the central metabolism of *A. niger* (Fig. 1) was used in combination with metabolic flux ratio analysis (Zamboni et al., 2005) to estimate the *in vivo* metabolic fluxes from ^{13}C labeling data of proteinogenic amino acids measured by GC–MS, extracellular rates, and anabolic fluxes. Subsequently, elementary flux mode analysis was applied to the same metabolic network to study the overall flux space for various levels of production.

The integration of *in vivo* and *in silico* fluxes allowed a quantitative prediction of novel targets for strain engineering, fully considering the already realized optimization.

2. Materials and methods

2.1. Strains and maintenance

The *A. niger* wild type SKANip8 and the recombinant strain *A. niger* SKAn1015 were used in this work (Zuccaro et al., 2008). The latter expresses the *suc1* gene, encoding fructofuranosidase, under the control of the constitutive *pki*A (pyruvate kinase)

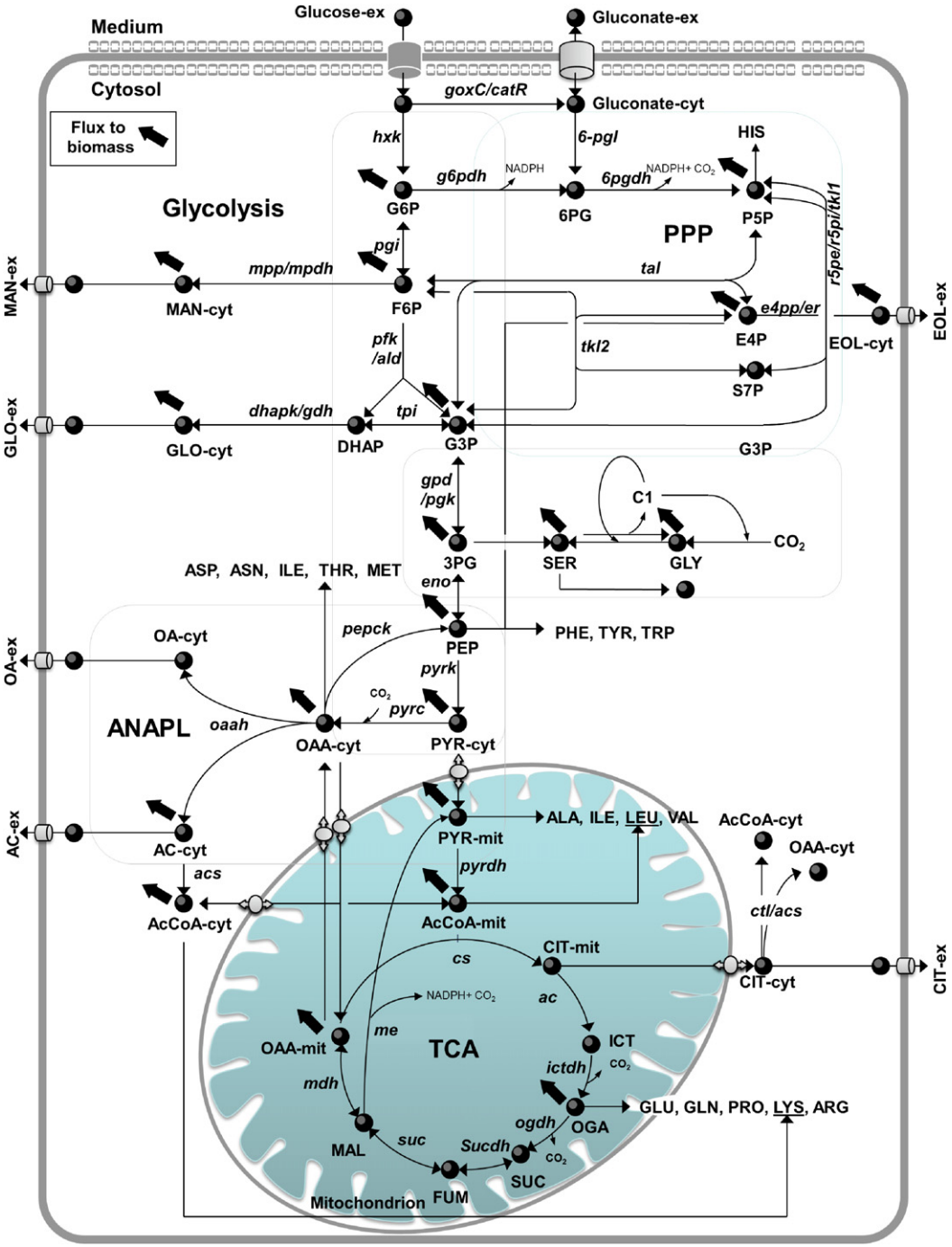

Fig. 1. Compartmented metabolic network of *Aspergillus niger*. For abbreviations of the intermediates see supplementary material.

promoter (Zuccaro et al., 2008). Both strains were maintained as frozen spore suspension in 50% glycerol at −80 °C.

2.2. Medium

The cultivation medium contained per litre: 15 g glucose, 20 mL salt solution (50× with 180 g/L $NaNO_3$, 10 g/L KCl, 30 g/L KH_2PO_4, 10 g/L $MgSO_4 \cdot 7H_2O$) and 1 mL trace element solution (1000× with 10 g/L EDTA, 4.4 g/L $ZnSO_4 \cdot 7H_2O$, 1.5 g/L $MnCl_2 \cdot 4H_2O$, 0.32 g/L $CuSO_4 \cdot 5H_2O$, 7.5 g/L $FeSO_4 \cdot 7H_2O$, 0.32 g/L $CoCl_2 \cdot 6H_2O$, 1.47 g/L $CaCl_2 \cdot 2H_2O$ and 0.22 g/L $(NH_4)_6Mo_7O_{24} \cdot 4H_2O$). It was based on a previous medium (pH 5) for optimum fructofuranosidase production in *A. niger* (Driouch et al. 2010a) with slight modifications (e.g. lower glucose) for the cultivation studies here. The basal medium and the stock solutions for salt and trace elements were autoclaved separately for 20 min at 121 °C and cooled down to room temperature prior to mixing. In ^{13}C-labeling experiments, glucose was replaced by an equimolar amount of ^{13}C-labeled glucose. To resolve the metabolic fluxes of interest two parallel set-ups were chosen for the labeling studies (Wittmann and Heinzle 2002). This included one set-up with [1-^{13}C] glucose (99%, Cambridge Isotope Laboratories, Andover, USA) and one set-up with a 1:1 mixture of [$^{13}C_6$] glucose (99%, Cambridge Isotope Laboratories, Andover, USA) and naturally labeled glucose.

2.3. Cultivation

A spore inoculum of *A. niger* was prepared by incubating thawn spores from the glycerol stock at 30 °C for 3 day on 30 g/L potato dextrose agar (Sigma-Aldrich, Seelze, Germany). Spores were then harvested as suspension by spreading 20 mL sterile 0.9% NaCl solution over the plate. After filtration of the suspension (Miracloth, 25 μm pore size, CalBioChem, Darmstadt, Germany) the obtained spore concentration was quantified photometrically at 600 nm considering a correlation factor of 1 $OD_{600} = 1.16 \times 10^7$ spores/mL, which had been determined experimentally. Liquid cultures were then inoculated to an initial spore concentration of $< 1\%$ of final cell dry weight. All cultivations were performed in three independent replicates using 250 mL baffled shake flasks with 25 mL medium on a rotary shaker (Certomat BS-1/50 mm, Sartorius, Göttingen, Germany) at 37 °C and 240 rpm.

2.4. Labeling analysis of proteinogenic amino acids by GC–MS

Cells of *A. niger* were harvested during mid-exponential growth by filtration of 5 mL culture broth through a cellulose acetate filter (pore size 20 μm, Sartorius, Göttingen, Germany). After removal of excess medium by two washing steps with sterile 0.9% NaCl solution, the cells were frozen in liquid nitrogen and then lyophilized at −60 °C (Alpha 1-4 LD, Christ GmbH, Osterode, Germany). For protein hydrolysis 10 mg of lyophilized biomass was incubated in 400 μL of 6 M HCl at 100 °C for 24 h. After pH adjustment to 7.0 by 6 M NaOH, the hydrolysate was clarified (0.2 μm, Ultrafree MC, Millipore, Bedford, MA, USA) and again lyophilized. The contained proteinogenic amino acids were then converted into *t*-butyl-di-methyl-silyl derivates (Wittmann et al., 2002). Their labeling pattern was quantified by GC–MS (HP 6890, M 5973, Agilent Technologies, Waldbronn, Germany) as described previously (Kiefer et al., 2004). All samples were measured first in scan mode, therewith excluding isobaric overlay (Wittmann, 2007). The relative fractions of the mass isotopomers of interest were then determined in duplicate in selective ion monitoring (SIM) mode.

2.5. Analysis of substrates and products

Cell dry weight (CDW) was determined in triplicate. For this purpose, 10 mL of broth was filtered through a pre-weighted cellulose acetate filter (pore size 20 μm, Sartorius, Göttingen, Germany). Subsequently, the filter was rinsed twice with 5 mL deionized water and dried at 100 °C until weight constancy. After cooling in a desiccator, the cell dry weight was determined by gravimetrically. The quantification of polyols (mannitol, erythritol and glycerol) and organic acids (oxalate, acetate, butyrate, lactate, propionate and gluconate) in cultivation supernatant, obtained by filtration (Minisart 0.2 μm, Sartorius, Göttingen, Germany), was carried out in duplicate on a HPLC (Elite Lachrome HITACHI Ltd., Japan) with a Metacarb 67 H column (250 mm × 4.6 mm, 5 μm, VWR-Hitachi International GmbH, Darmstadt, Germany) and 1 mM H_2SO_4 as mobile phase at a flow rate of 0.8 mL/min and 70 °C. The detection was performed with a UV detector (210 nm). Glucose concentration was determined in duplicate in filtered culture supernatant using a glucose analyzer (Biochemistry Analyze, YSI, OH, USA).

2.6. Elemental composition of biomass

Cells of *A. niger* were harvested by filtration of 5 mL culture broth through a cellulose acetate filter (pore size 20 μm, Sartorius, Göttingen, Germany). After removal of excess medium by two washing steps with sterile 0.9% NaCl solution, the washed cell pellet was frozen in liquid nitrogen and then lyophilized at −60 °C (Alpha 1-4 LD, Christ GmbH, Osterode, Germany). Subsequently, the dry biomass was weighed and then analyzed with a CHNS Analyzer (Elementar Analysensysteme GmbH, Hanau, Germany) using acetanilide as internal reference.

2.7. Protein concentration in culture supernatant

The total protein concentration in culture supernatant was determined in triplicate by the bicinchoninic acid method using bovine serum albumin as external standard (BSA protein assay kit, Pierce, Rockford, IL, USA) following the instruction given by the distributor. For this purpose, 5 mL broth samples were filtered (cellulose acetate filter, pore size 20 μm, Sartorius, Germany) and clarified by centrifugation (13,000*g*, 10 min, 4 °C) prior to analysis.

2.8. Extracellular protein pattern

Sodium dodecyl sulfate-polyacrylamide gel electrophoresis (SDS-PAGE) was used to separate the secreted proteins in culture supernatant samples. First, 170 μL culture supernatant was mixed with 830 μL acetone for protein precipitation. The obtained pellet was dried and re-suspended in 10 μL buffer following the instruction given by the distributor. A volume of 3 μL (corresponding to 50 μL culture supernatant) was then loaded onto a 4–12% Bis-Tris-Mini Gel (Novex Mini-Cell 1 mm, 15-well, Invitrogen, Karlsruhe, Germany) for protein separation. The applied molecular mass marker was the PageRuler Unstained Protein Ladder (SM0661, Fermentas, St. Leon-Rot, Germany). The gel was scanned using the Molecular Imager® PharosFX System (BioRad, Munich, Germany). The volume of each protein band was then determined by the 1-D Analysis Software (Version 4.6.9, BioRad, Munich, Germany). Hereby, the glycosylated fructofuranosidase exhibited a band at about 110–120 kDa (Zuccaro et al., 2008).

2.9. Fructofuranosidase concentration in culture supernatant

The relative amount of fructofuranosidase among all proteins in the supernatant was determined via the relative volume of the corresponding band on the protein gel, normalized to the total volume of all bands. The relative amount of fructofuranosidase, together with the total protein concentration (see above), then yielded the concentration of this protein in the supernatant.

2.10. Fructofuranosidase activity

The specific activity of secreted fructofuranosidase was determined in the supernatant of cultivation broth, obtained by filtration of 5 mL broth through a cellulose acetate filter (pore size 20 μm, Sartorius, Göttingen, Germany) and subsequent centrifugation (13,000*g*, 10 min, 4 °C). The collected supernatant was immediately used for determination of fructofuranosidase enzyme activity as described previously (Driouch et al., 2010a).

2.11. Metabolic reaction network

A compartmented metabolic network model of *A. niger* was constructed on basis of validated models recently described (Andersen et al., 2008; Jouhten et al., 2009; Meijer et al., 2009; Melzer et al., 2009). Briefly, the network included all major central pathways, such as the glycolysis, the pentose phosphate pathway (PPP), the gluconeogenic and the anaplerotic pathways, the tricarboxylic acid (TCA) cycle, and the glyoxylate pathway, the anabolic metabolism, the biosynthetic route towards the recombinant fructofuranosidase as well as the reactions involved in substrate uptake and by-product formation (Fig. 1). The cytosol and the mitochondrion were considered as separate compartments. This included separate pools for pyruvate, oxaloacetate and acetyl-CoA in both compartments. The transport of pyruvate into the mitochondrion was considered to be unidirectional. However, the transport of oxaloacetate and acetyl-CoA into the mitochondria was regarded reversible and a priori to be bi-directional. The compartmentation of anabolism, including amino acid biosynthesis, was revised by inspection of metabolic flux studies on different yeasts and fungi. This revealed that the central carbon metabolism of yeast such as *Saccharomyces cerevisiae* (Blank et al., 2005; Blank and Sauer, 2004; Fiaux et al., 2003), *Pichia anomola* (Fredlund et al., 2004), *Pichia stipitis* (Fiaux et al., 2003), *Pichia pastoris* (Sola et al., 2004) and fungi such as *Trichoderma reesei* (Jouhten et al., 2009) is rather similar and conserved with respect to pathway reactions and their localization, despite variations with respect to its regulation. The metabolic reaction network consisted of 46 irreversible and 11 reversible reactions and 28 intracellular metabolites (Fig. 1). A detailed overview on the model including all reactions is provided in the supplementary material (see S1).

2.12. Metabolic flux calculation

The estimation of metabolic fluxes was performed with the MATLAB-based program FiatFLUX 1.67, which was kindly provided by the authors (Zamboni et al., 2005). This software package consists of two modules for (i) computation of metabolic flux ratios for ^{13}C-labeling data and (ii) estimation of net carbon fluxes within a comprehensive model of metabolite balances from determined metabolic flux ratios, measured extracellular fluxes and biomass requirement. Shortly, the proteinogenic amino acids are synthesized from one or more metabolic intermediates. A detailed description of the principle and the evaluation of flux ratios from MDV_M of metabolic intermediates is given elsewhere (Fredlund et al., 2004; Zamboni et al., 2005). For flux calculation in the present work, the obtained mass isotopomer distributions of the derivatized amino acids alanine, glycine, valine, leucine, isoleucine, proline, serine, threonine, phenylalanine, aspartate, glutamate, histidine, lysine and tyrosine were corrected for natural abundance of stable isotopes. Due to the low inoculum level the potential interference of non-labeled carbon from the inoculum could be neglected. The potential influence of non-labeled carbon dioxide from ambient air was considered. For flux calculation, the metabolic flux ratios were first determined by the flux ratio module and then used on basis of the metabolic reaction network with 46 reactions and 28 metabolites to obtain the net fluxes. For this purpose, the metabolic fluxes were calculated using (i) the stoichiometric reaction matrix, (ii) calculated metabolic flux ratios as additional constraints for the stoichiometric equation system, (iii) measured time-averaged uptake and production rates of external metabolites and (iv) information on precursor requirements for biomass synthesis (Andersen et al., 2008; Meijer et al., 2009; Melzer et al., 2009).

2.13. Elementary flux mode analysis

Elementary flux mode calculation was performed on basis of a large-scale model condensed from the genome-scale network model of *A. niger* (Andersen et al., 2008) as described recently (Melzer et al., 2009). In addition to the previous calculations, the network model was extended to account for pathways towards potential by-products, i.e. gluconate, oxalate, mannitol, erythritol and glycerol. The corresponding metabolic network reactions are listed in the supplementary material (see S1). On basis of the determined elementary modes, a detailed investigation of metabolic network properties was carried out. This included the estimation of theoretical (maximum) yields, relative fluxes through intracellular metabolic pathways and target prediction for strain engineering. Calculations were partially automated and implemented into Matlab (Mathworks Inc., Natick, MA) and evaluated in Excel (Microsoft Office, Windows, 2007).

3. Results

3.1. Growth and production performance of A. niger

The effect of fructofuranosidase expression on the metabolism of *A. niger* was assessed in comparative batch cultures of the wild type strain SKANip8 and the producer SKAn1015 (Fig. 2A and B). After an initial phase of spore germination, both strains grew exponentially with a specific growth rate of 0.17 h^{-1}. Glucose as sole carbon source was still available at the end of the process. The recombinant strain accumulated about 45 U/mL of fructofuranosidase within 18 h, whereas production in the wild type strain was negligible. Both strains differed quite markedly concerning the formation of gluconate. The producer accumulated 4 g/L of this by-product, which was twice as much as observed for the parent strain. Oxalate was secreted only in minor amounts and at similar levels for both strains. Polyols such as mannitol, erythritol or glycerol were not formed, indicating fully aerobic conditions during all cultivations. Overall, the three biological replicates for each strain exhibited high agreement, which underlines the consistency of the data (Fig. 2A and B). Electrophoretic analysis of the culture supernatant reflected that fructofuranosidase (120 kDa) was the dominating protein (Fig. 3). It accounted for 95% of the total protein excreted by the producer. Taking the total protein concentration in the culture supernatant into account this corresponded to an enzyme titer of 0.11 g/L of fructofuranosidase (Table 1). In contrast, the reference strain did not exhibit the enzyme (Fig. 3) or corresponding activity (Fig. 2A).

3.2. Verification of metabolic and isotopic steady-state

A crucial pre-requisite for valid flux data in batch culture is pseudo-steady state. From batch cultures, this can be deduced from constant kinetic and stoichiometric characteristics of the cells, as well as from isotopic steady-state (Becker et al., 2008). Careful inspection of these data confirmed metabolic steady-state during the period studied. First, both strains cells grew exponentially with a

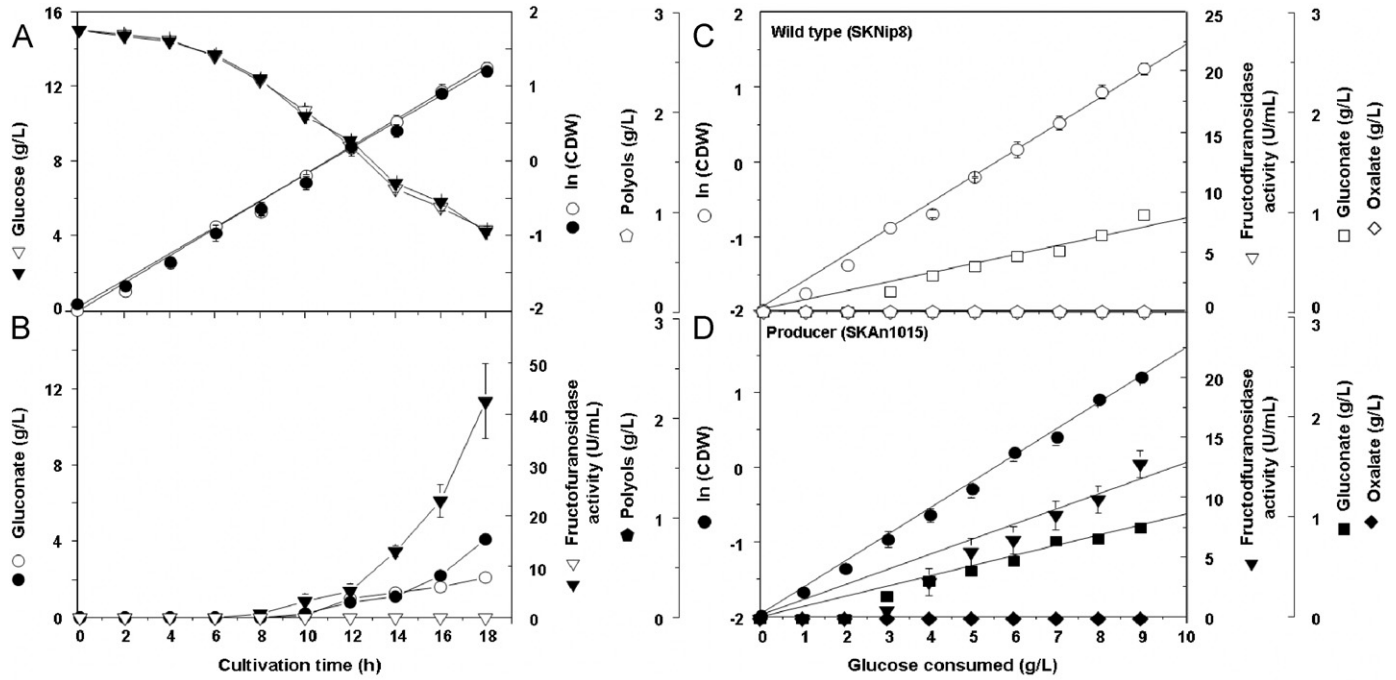

Fig. 2. Cultivation profile of *Aspergillus niger* SKANip8 (wild type) and SKAn1015 (recombinant fructofuranosidase producer) on glucose minimal medium. Open symbols reflect the wild type, solid symbols the recombinant strain. The data given represent mean values and deviations from three replicate cultures for each strain.

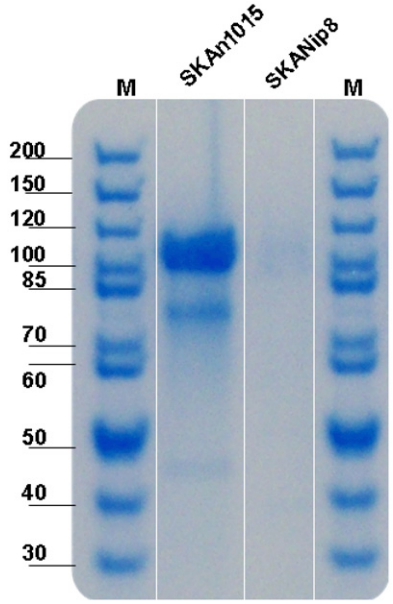

Fig. 3. Sodium dodecyl sulfate-polyacrylamide gel electrophoresis (SDS-PAGE) analysis of culture supernatant from *Aspergillus niger* SKANip8 and SKAn1015. The left lane (M) shows the molecular weight marker. The strong band at about 110-120 kDa for the recombinant producer corresponds to fructofuranosidase (Zuccaro et al., 2008).

constant specific growth rate (Fig. 2A). Moreover, the yield coefficients for growth and by-products remained constant over time as indicated by their linear correlation to the consumed substrate (Fig. 2C and D). The elemental composition of the biomass did not vary between the two strains and also stayed constant throughout the cultivation (Table 2). Isotopic steady-state was proven by constant labeling patterns of the proteinogenic amino acids and deduced constant metabolic flux ratios during at different time points of the cultivation (see S2). Overall, all data clearly indicated steady-state conditions so that flux analysis was feasible.

Table 1
Kinetics and stoichiometry of *Aspergillus niger* SKANip8 (wild type) and SKAn1015 (recombinant fructofuranosidase producer) during batch cultivation on glucose and nitrate. The data represent three replicates for each strain with corresponding deviations and refer to the culture profile shown in Fig. 2A–D.

	SKANip8 Wild type	**SKAn1015 Producer**
Cell dry weight (g/L)	3.50 ± 0.40	3.30 ± 0.40
Specific growth rate (h^{-1})	0.17 ± 0.02	0.17 ± 0.01
Biomass yield on glucose (g/g)	0.37 ± 0.02	0.33 ± 0.01
Spec. glucose uptake rate (mmol/g*h)	1.13 ± 0.02	1.17 ± 0.01
$Fructofuranosidase\ activity_{extracellular}$ (U/mL)	0 ± 0	43 ± 6
Spec. fructofuranosidase activity (U/mg)	0 ± 0	13 ± 3
$Fructofuranosidase\ concentration_{extracellular}$ (g/L)	0 ± 0	0.11 ± 0

Table 2
Elemental composition of *Aspergillus niger* SKANip8 (wild type) and SKAn1015 (recombinant fructofuranosidase producer) at different time points of the cultivation. The data given are ratios of carbon to nitrogen (C/N), carbon to hydrogen (C/H) and carbon to sulfur (C/S).

	C/N	**C/H**	**C/S**
SKNip8			
12 h	6.5	7.6	103
16 h	6.4	7.6	109
18 h	6.4	7.4	88
Average	**6.4 ± 0.0**	**7.5 ± 0.1**	**100 ± 11**
SKAn1015			
12 h	6.3	7.3	81
16 h	6.5	7.5	100
18 h	6.3	7.7	103
Average	**6.4 ± 0.1**	**7.5 ± 0.2**	**95 ± 12**

3.3. Metabolic pathway fluxes in the wild type of A. niger

The central carbon metabolism of *A. niger* was first studied by metabolic flux ratio analysis (METAFoR) comprising parallel isotope experiments on 99% [1-^{13}C] and 50% [$^{13}C_6$] glucose. Metabolic flux ratios were estimated from the labeling data of proteinogenic amino acids (see S3) at different time points of the cultivation. A qualitative inspection of the data revealed that *A. niger* exhibited simultaneous contribution of glycolysis and PPP to the break-down of glucose (Table 3). The strain showed significant activity of the TCA cycle. Mitochondrial malic enzyme was inactive, indicating the PPP as major source for NADPH. Also, cytosolic phosphoenolpyruvate carboxykinase was found inactive. The overall flux distribution was estimated on basis of the compartmented stoichiometric model of the *A. niger* metabolism (see S1), the measured extracellular rates (Table 1), the metabolic flux ratios as ^{13}C-constraints (Table 3) and known precursor requirements for anabolism and fructofuranosidase biosynthesis (see S1). For the calculation, the corresponding time averaged yield coefficients and rates (Table 1) as well as the GC–MS labeling data (see S3) of the cultivation were considered. For both strains the same biomass composition was assumed, which was justified by the excellent agreement of the cellular composition (Table 2). Due to substantial formation of gluconate, the wild type of *A. niger* directed only 75% of the up-taken glucose into the central metabolism (Fig. 4). At the G6P node, the dominating fraction of carbon entered into glycolysis. The flux into the PPP was obviously higher than the flux withdrawing carbon from this pathway for anabolism. Due to this, a substantial amount of carbon was redirected back into the glycolytic chain at the level of F6P and G3P. Pyruvate was the major precursor transported into the mitochondrion. At lower level, oxaloacetate was exchanged between the two compartments. *A. niger* revealed an oxidative metabolism with cyclic operation of the TCA cycle.

Table 3
Metabolic flux ratios of the wild type *Aspergillus niger* SKANip8 and the fructofuranosidase producing strain *Aspergillus niger* SKAn1015 obtained from [1-^{13}C] and [U-^{13}C] glucose experiments. Abbreviations: lb, lower bound; up, upper bound; *tkl*, transketolase; *tal*, transaldolase; *pepck*, PEP carboxykinase; *me*, malic enzyme; n.d., not detectable because the fragment needed for tracing this activity was absent; SD, standard deviation. For abbreviations of the intermediates see the supplementary material.

Strains	Fraction of total pool (%) (mean ± SD)	
	SKANip8 (wild type)	SKAn1015 (producer)
Glycolysis and PP pathway		
SER through glycolysis	33 ± 2	45 ± 1
R5P from G6P (lb)	24 ± 2	35 ± 2
R5P from T3P and S7P (*tkl* reaction)	35 ± 3	45 ± 4
R5P from E4P (*tkl*/*tal* reaction)	45 ± 3	50 ± 3
E4P from TK	73 ± 5	46 ± 2
C1-metabolism		
SER from GLY	48 ± 1	35 ± 1
GLY from SER	67 ± 1	65 ± 2
Labeled CO_2	13 ± 3	18 ± 1
Glycolysis, ANAPL and TCA cycle		
PEP-cyt from OAA-cyt (*pepck*)	0 ± 0	0 ± 0
OAA-cyt from PYR-cyt	80 ± 4	80 ± 1
AcCoA-mit from PYR-mit	n. d.	101 ± 2
OAA-mit from ANAPL	54 ± 4	75 ± 1
OAA-mit from ANAPL (old)	43 ± 2	73 ± 1
PYR-mit from MAL (*me*, up)	0 ± 0	78 ± 2
PYR-mit from MAL (*me*, lb)	0 ± 0	81 ± 3

3.4. Response of metabolic fluxes to recombinant fructofuranosidase production

The recombinant strain exhibited a significant redirection of fluxes (Fig. 4). The relative flux towards gluconate was almost doubled, significantly reducing the amount of glucose entering central metabolism. The production of fructofuranosidase was further linked to an up-regulation of the relative flux into the PPP, whereas the relative flux into the glycolysis was strongly decreased at the level of phosphoglucoisomerase. As a result, the overall flux entering the cytosolic pyruvate pool was reduced by more almost 50%. This caused a significantly decreased TCA cycle flux in the recombinant strain. Interestingly, malic enzyme in the mitochondrion was active in contrast to the wild type. The flux distribution through other reactions were found similar between the two strains. Cytosolic phosphoenolpyruvate carboxykinase was found inactive.

3.5. Correlation of in vivo pathway fluxes with improved production performance

The two flux data sets were now analyzed to extract the changes that were most significantly linked to improved production of fructofuranosidase. For this purpose, flux correlation coefficients (α_{vivo}) were extracted from the flux data sets of the two compared *Aspergillus* strains (Eq. (1)). These coefficients quantify the correlation of a single flux in the network (v_i) with a target flux (v_j), in this case the flux of fructofuranosidase production

$$\alpha_{vivo} = \frac{\mathrm{cov}(v_j, v_i)}{\delta_j^2} \quad (1)$$

The calculation quantifies the flux response to the metabolic burden of product formation. Hereby, it allows to differentiate between increased ($\alpha_{vivo} > 0$), decreased ($\alpha_{vivo} < 0$) and unaffected ($\alpha_{vivo} = 0$) reactions. As already obvious from visual inspection of the flux maps, the correlation coefficients indicated the activation of the PPP, the increased formation of gluconate, as well as the decreased fluxes through glycolysis or TCA cycle (Table 4). It should be noticed that the linear correlation analysis could only be based on two data sets, which might weaken it to a certain extent. The precision of the estimated fluxes, however, was rather high (Fig. 4) that it still appeared meaningful to explore the data in the proposed way.

3.6. In silico pathway analysis of recombinant fructofuranosidase production

Based on previous simulations (Melzer et al., 2009), structural properties of the metabolic network of *A. niger* for production of fructofuranosidase were studied by elementary flux mode analysis. With glucose as carbon and nitrate as nitrogen source, 109,661 different elementary modes resulted for the compartmented network. These spanned the whole space of fluxes theoretically possible. The modes differed substantially in the corresponding yield for the enzyme or the biomass. The dominating fraction of modes was linked to exclusive production of either fructofuranosidase or biomass (Fig. 5). Simultaneous formation of biomass and fructofuranosidase was observed only for 3% of the modes (2950). Interestingly, most of these modes were located quite close to the line of optimality connecting the extreme modes for maximum theoretical production of biomass or enzyme, respectively. Overall, 43% of the modes (47,508) enabled fructofuranosidase production. The maximum theoretical carbon yield for the enzyme was 0.61 C-mol/C-mol. The corresponding

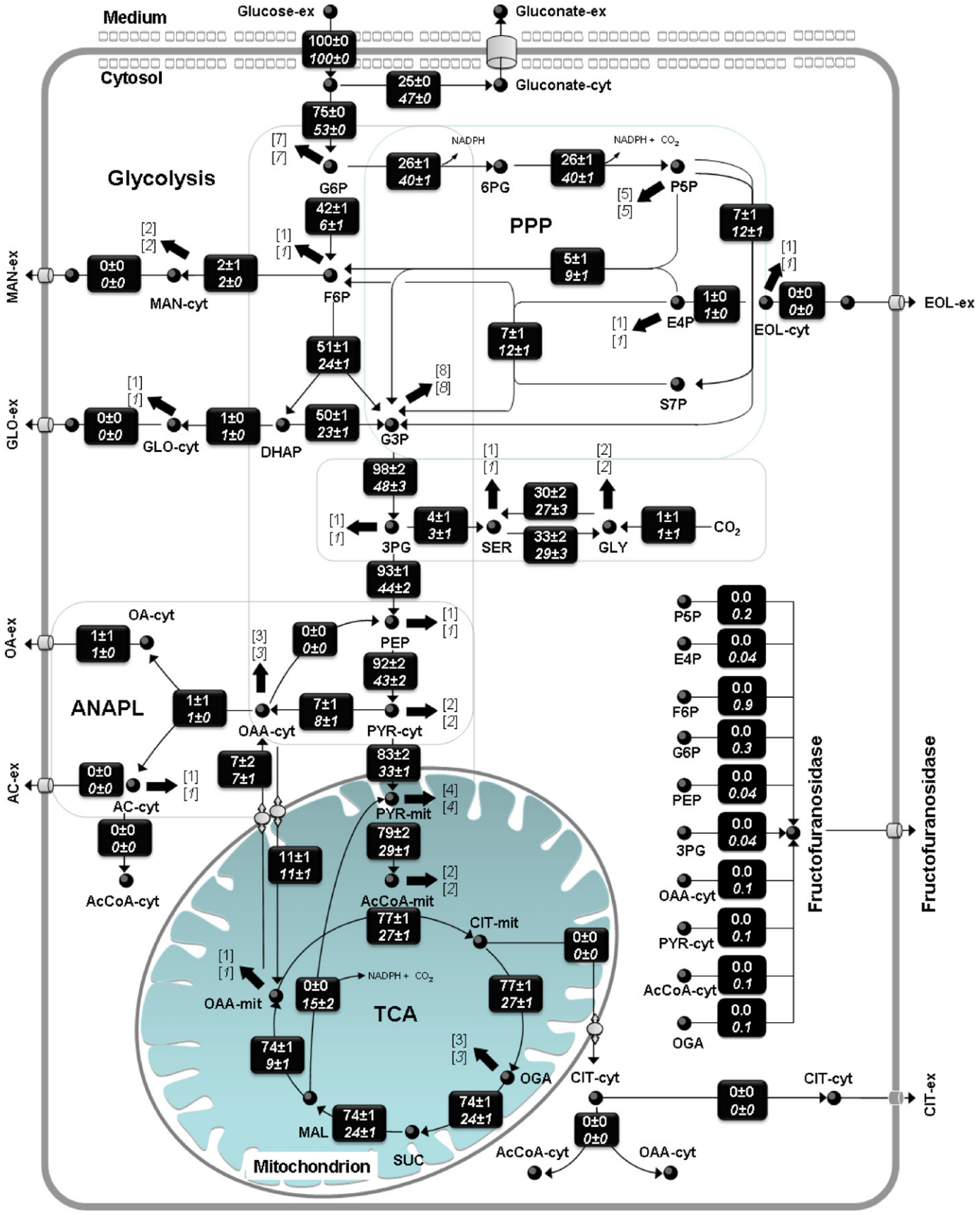

Fig. 4. Metabolic flux distribution of *Aspergillus niger* SKANip8 (wild-type, top) and SKAn1015 (recombinant fructofuranosidase producer, bottom) on glucose minimal medium. All fluxes are normalized to the specific glucose uptake rate, which was 1.13 ± 0.02 mmol/g/h for the wild type and 1.17 ± 0.01 mmol/g/h for the producer (Table 1). The corresponding set of reactions and abbreviations of the underlying stoichiometric model is listed in the supplementary material S1.

Table 4
Flux correlation coefficients *in silico* and *in vivo* deduced from ^{13}C flux data (Fig. 4) and elementary flux mode analysis (Fig. 5) for *Aspergillus niger* producing fructofuranosidase.

Reaction	Gene	AngXX	$\alpha_{in\ vivo}$	$\alpha_{in\ silico}$
Gluconate				
Glucose oxidase	*goxC*	An01g14740	22	−12
EMP				
Hexokinase	*hxk*	An02g14380	−1	0
Glucose 6-phosphate isomerase	*pgi*	An16g05420	−36	−8
Phosphofructokinase	*pfkA*	An18g01670	−27	−33
Fructose-bisphosphate aldolase	*fda*	An02g07470	−27	−33
Triosephosphate isomerase	*tpiA*	An02g04920	−27	−3
Glyceraldehyde 3-phosphate dehydrogenase	*gpd*	An16g01830	−50	−4
Phosphoglycerate kinase	*pgk*	An08g02260	−50	−4
Enolase	*enol*	An18g06250	−49	−5
Pyruvate kinase	*pkiA*	An07g08990	−49	−21
POL				
Mannitol 1-phosphate dehydrogenase	*mpdh*	An06g00750	0	−2
Erythrose 4-phosphate phosphatase	*e4pp*	An01g06970	0	−0.2
PPP				
Glucose 6-phosphate dehydrogenase	*zwf*	An02g12140	14	20
Phosphogluconate dehydrogenase	*gnd*	An11g06120	14	20
Ribulose 5-phosphate epimerase	*rpe*	An11g02040	10	3
Ribulose 5-phosphate isomerase	*rpi*	An02g02930	10	3
Transketolase	*tkt1*	An02930	10	3
Transaldolase	*tal*	An07g03850	4	2
Transketolase	*tkt2*	An08g06430	4	2
PYRM				
Pyruvate carboxylase	*pyc*	An04g02090	1	−17
Phosphoenolpyruvate carboxykinase	*pckG*	An05g02550	0	−15
Oxalacetate hydrolase	*oahA*	An10g00820	1	−3
Malic enzyme	*mez*	An12g00160	15	−5
TCA				
Pyruvate dehydrogenase	*pyrdh*	An07g09530	−50	−11
Citrate synthase	*citA*	An09g06680	−50	−78
Isocitrate dehydrogenase	*icdA*	An08g05580	−50	−4
Oxoglutarate dehydrogenase	*ogahA*	An08g02970	−50	−8
Succinate dehydrogenase	*sucD*	An14g04395	−50	−11
Fumarate hydratase	*fumC*	An12g07850	−50	−7
Malate dehydrogenase	*mdh*	An07g03850	15	−11

mode was located the upper left corner of the triangle (indicated as C in Fig. 5).

3.7. Correlation of in silico pathway fluxes with improved production performance

The elementary modes contained a large set of unique *in silico* flux distributions reflecting various metabolic states. With respect to the optimization of fructofuranosidase production, only the enzyme producing modes appeared relevant. A closer look revealed that most of them did not produce biomass, but only different levels of by-products. The production of the recombinant enzyme, however, was obviously growth coupled (Fig. 2), i.e. was characterized by simultaneous formation of biomass and fructofuranosidase. Due to this, the sub set of elementary modes with simultaneous production of enzyme and biomass most closely matched the phenotype of the investigated strains. This sub set was therefore selected to extract, how *in silico* fluxes correlate with the production of the recombinant enzyme. For this purpose, flux correlation coefficients (α_{silico}), quantifying the correlation of a single flux in the network (v_i) with the target flux (v_j), i.e. fructofuranosidase production, were estimated via correlation analysis of the corresponding elementary modes

$$\alpha_{silico} = \frac{\mathrm{cov}(v_j, v_i)}{\delta_j^2} \quad (2)$$

Overall, a quite diverse picture resulted for the different reactions of the *A. niger* network (Table 4). Many reactions correlated with production. Positive values exclusively resulted for the PPP reactions, most significant for the entry step catalyzed by glucose 6-phosphate dehydrogenase. This indicates that the corresponding fluxes through the PPP increase with higher fructofuranosidase production. Many reactions revealed the opposite behavior. The negative correlation of the flux through citrate synthase in the TCA cycle was most pronounced. In addition, the simulation predicted a decrease of the fluxes through phosphofructokinase, pyruvate kinase and pyruvate carboxylase linked to improved formation of the target enzyme. A third fraction of reactions were obviously not affected and showed values of α_{silico} close to zero.

4. Discussion

The filamentous fungus *Aspergillus niger* is an important industrial producer of extracellular enzymes (Lubertozzi and Keasling, 2009). This explains the huge interest in its metabolic properties towards superior production strains. The recombinant strain *A. niger* SKAn1015 studied here revealed efficient secretion of fructofuranosidase, an enzyme of high relevance as biocatalyst for the supply of probiotic rare sugars (Maiorano et al., 2008). As shown the organism was capable to maintain its overall growth behavior, e.g. specific rates of growth or substrate uptake, despite

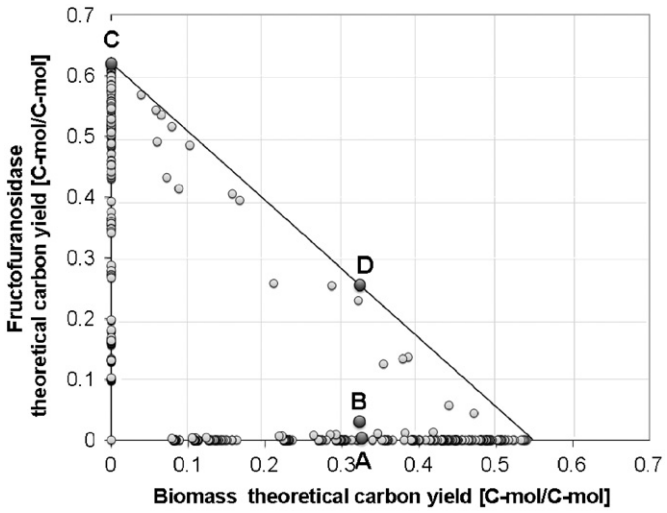

Fig. 5. Metabolic states of *Aspergillus niger* assessed from *in vivo* and *in silico* flux analysis. The data comprise the set of elementary modes, represented by the open circles, for fructofuranosidase and biomass production on glucose and nitrate (Melzer et al. 2009). The solution space of the elementary modes is marked as the interior and the sides of the rectangular triangle. The modes on the two axes represent extreme modes exclusively linked to production of fructofuranosidase (*y*-axis) or biomass (*x*-axis). Additionally, the experimentally observed metabolic flux states of the wild type *A. niger* SKANip8 (A) and the recombinant strain *A. niger* SKAn1015 (B) are shown. The other states reflect the theoretical optimum production for fructofuranosidase at zero growth (C) and at the biomass yield observed for the producing strain (D).

the significant cellular burden for biosynthesis of the large, highly glycosylated protein. Fluxome analysis by ^{13}C labeling experiments was carried out to study the cellular response in more detail. Careful revision of the data (Tables 1–3, Fig. 2, supplement S3) confirmed the presence of isotopic and metabolic steady-state in the batch cultures so that the chosen ^{13}C flux approach appeared well suited. The elemental composition was identical between the two strains (Table 2) and also in good agreement with previous measurements from filamentous fungi (Nielsen and Villadsen, 1994). Since any significant alteration of the macromolecular composition, e.g. on the level of protein, lipids, DNA, RNA or carbohydrates, would have directly affected these values (Nielsen and Villadsen, 1994), it was justified to assume the same biomass composition for the two strains.

The cells responded to the production by a redistribution of fluxes through central pathways, which provided interesting insights into the underlying metabolic network. It should be noted, that due to similar values for the specific glucose uptake rate, all conclusions drawn for the relative flux distribution, also hold for absolute fluxes. All of the observed changes were mediated through passive adaptation of the network, because the expression of the recombinant *suc1* gene, encoding for fructofuranosidase was the sole genetic perturbation performed. In addition, elementary flux mode analysis provided a detailed view on theoretical flux scenarios at various production levels. As shown below, the integration of the *in vivo* flux data with the *in silico* flux space can create an interesting design space for strain engineering, which relates the real behavior of the studied strains to the ideal blueprints of optimum producers.

4.1. Redox metabolism

Most strikingly, the production of the recombinant enzyme was accompanied by elevated relative fluxes through the cytosolic PPP and the mitochondrial malic enzyme. An increased PPP flux was also observed for amylase-producing strains of *Aspergillus oryzae*, when compared to the wild type suggesting a more general feature of recombinant filamentous fungi (Pedersen et al., 1999). PPP and malic enzyme supply the cofactor NADPH. NADPH is particularly required for the biosynthesis of amino acids as building blocks for proteins. This suggests that the increased fluxes might reflect the extra demand for the biosynthesis of fructofuranosidase. *A. niger* produced 0.11 g/L of the target enzyme (Table 1). At the same time the fungus synthesized 0.86 g/L cellular protein as part of the biomass. The latter value results from the concentration of biomass (Table 1) and its protein content 0.26 g/g (Andersen et al., 2008). Fructofuranosidase obviously roughly accounted for 13% of the total cellular protein, which indeed poses a significantly increased NADPH demand. Due to this the flux changes for NADPH supplying reactions at least partly reflect the increased demand for this cofactor in the recombinant strain. The flux increase through the cytosolic PPP and the mitochondrial malic enzyme result in a relative increase of 43% for the NADPH supply by these two pathways as compared to the wild type. This is higher than the actual extra demand for this cofactor for biosynthesis of recombinant protein, also taking into account that a certain fraction of the protein is composed of glycosylation residues, not demanding for NADPH during biosynthesis This indicates a more complex picture. It is possible, that through activation of PPP and malic enzyme the recombinant strain even generates an apparent excess for NADPH. Such behavior has been previously observed for other microorganisms (Wittmann and Heinzle 2002). Here, it could be due to the use of extra NADPH for protein folding and possible ER stress in connection with secreting the recombinant protein. Considering that one of the isoenzymes for isocitrate dehydrogenase generates NADPH, the reduced flux through the TCA cycle in the producer could also be associated to a decreased supply of this cofactor in the mitochondrion. Due to this the activation of the malic enzyme could partly compensate for the reduced NADPH supply by the TCA cycle. Nitrate, used as nitrogen source, requires substantial amounts of NADPH for reduction to ammonia (Diano et al., 2006). The assimilation of nitrate thus competes for NADPH with the production of the enzyme. Interestingly, nitrate leads to higher enzyme titres as compared to ammonia (Driouch et al., 2010a). This might be an indication of so far unknown regulatory mechanisms.

4.2. PPP and TCA cycle as key switch points in the metabolism of filamentous fungi

Both strains revealed strong differences in the fluxes through PPP and TCA cycle. The comparison with data sets from other *Aspergilli* (see S4) illustrates that the flux pattern observed here, i.e. the changing contribution of the PPP and the TCA cycle displays a general feature of the underlying carbon core metabolism. Among various reactions of the central metabolism, these two pathways reveal the highest flexibility and obviously play a central role for the cells to cope with different environments or cellular burdens. As example, the relative PPP flux can increase to almost 60%, as observed for glucoamylase producing *A. niger* during batch cultivation (Pedersen et al., 2000), but can also exhibit low values of 20%, as reported here or from previous chemostat culture of *A. nidulans* (David et al., 2003) Notably, metabolic flexibility in yeasts Blank et al., 2005; Blank and Sauer, 2004) and bacteria (Wittmann and Heinzle 2002) is also mediated via flux adaptation through the PPP and the TCA cycle.

4.3. Remaining optimization potential for the recombinant strain

With regard to their production behavior the two investigated strains can be placed within the resulting flux space spanned by

elementary flux mode analysis. This results in the two metabolic states A (wild type) and B (producer). The wild type strain appears on the x-axis. The recombinant strain exhibits an improved yield as compared to its parent strain. It can be clearly seen that production is still far from the theoretical optimum. The distance between the actual flux state of the recombinant producer (B) and the theoretical optimum (C) suggests an enormous potential for future optimization. Obviously, the achieved fructofuranosidase yield of the producer displayed only 5% of the maximum potential, suggesting that further strain engineering appears generally promising.

4.4. Integration of in vivo and in vitro fluxes—competition between growth and production

It is typically observed that the formation of biomass and of a specific product, both demanding for carbon and nitrogen building blocks as well as redox power and energy, compete with each other . This can lead to decreased growth performance in strains with elevated production (Wittmann and Heinzle 2002). In the present work, the formation of fructofuranosidase was not related to negative effects on growth of *A. niger*. As example, the specific growth rate of the producing mutant was identical to that of the parent strain. The biomass yield was only slightly lower. The projection of the two strains into the flux space immediately explains this finding (Fig. 5). From a stoichiometric view point, the level of biomass yield observed for the wild type (A) and the producer (B) would even allow a significantly higher enzyme yield. The maximum enzyme production possible for the observed biomass yield of the recombinant strain is given by the metabolic state D, located on the boundary of the solution space. The corresponding fructofuranosidase yield of 0.24 C-mol/C-mol is about eightfold higher than the actually achieved value. This indicates that the production of fructofuranosidase could be increased eightfold without any limitation to be expected for growth. Only beyond this limit, optimization would be linked to reduced growth performance. This behavior is an inherent property of the metabolic network. As shown by the simulation, negative growth effects will be inherently caused by the imposed metabolic state at a certain point of development. Placed into the framework of the *in silico* flux space, this can be easily evaluated for any given strain. Clearly, negative growth effects would not necessarily indicate a wrong strain engineering strategy. Knowing the exact position for an existing strain and the corresponding points of optimality seems quite relevant for a metabolic engineer.

4.5. Integration of in vivo and in vitro fluxes for target prediction

The integration of *in vivo* physiology with *in silico* strain design can now be extended to the level of single fluxes. The flux correlation plot in Fig. 6 integrates all the information. The sectors II (upper right) and IV (lower left) mark areas of beneficial changes, i.e. they contain fluxes, which have changed into the desired (predicted) direction either as flux increase (sector II) or decrease (sector IV). It is remarkable that these two sectors contain by far the most fluxes. The overexpression of the enzyme was the only genetic change introduced, so all flux changes observed *in vivo* were a passive adaptation of the network. The picture in Fig. 6 highlights that many beneficial changes took place automatically. The fungus obviously readjusted its metabolism to a large extent towards the desired flux distribution way to support fructofuranosidase production. This can be regarded as a highly interesting response of *A. niger* to the metabolic burden of protein production—a key feature of this eukaryotic microorganism that could explain its high success in corresponding industrial applications. From their location in sectors II and IV, specific reactions appear as most relevant. These are globally distributed across the network and contained, e.g. *zwf/gnd* from the PPP, *citA* from the TCA cycle or *pfkA* from glycolysis. Other enzymes from the same pathways are of lower relevance. All these reactions, however, belong to the group that had inherently changed into the predicted direction. One might expect that they exhibit a certain natural capacity to allow even higher protein yields. Even more interesting with respect to future strain engineering are reactions in the opposed sector III. This sector reflects undesired phenotypic changes, i.e. a flux changes observed *in vivo*, which are the contrary of the optimally predicted solutions. Three prominent examples identified by this approach are malic enzyme

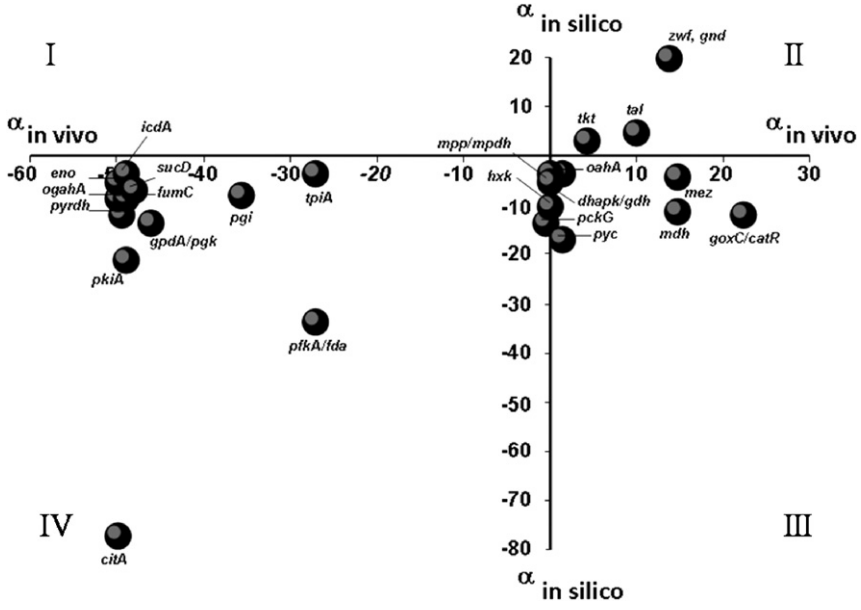

Fig. 6. Integration of *in silico* and *in vivo* pathway fluxes for strain design utilizing the concept of flux correlation coefficients. Shortly, the origin of the graph displays the starting point of the strain development—the non-producing wild type. The distance of each reaction from the origin in y-direction quantifies the outcome from the *in silico* simulations, i.e. a *recommended flux change*. This includes amplification targets (positive value) or attenuation targets (negative value) for optimization. At the same time, the distance from the origin in x-direction denotes the *realized flux change* for each reaction *in vivo*.

and malate dehydrogenase in the mitochondrion and gluconate over production. These three fluxes, obviously increased, despite a decrease, or even zero flux, is required for optimum performance. Although all pathways are linked to redox metabolism, the exact reason for their undesired change cannot be extracted from the present data. However, they all display interesting metabolic engineering targets. Their deletion or attenuation by direct genetic engineering could aid to bring the flux back towards the optimum distribution. Interestingly, no flux was found in sector I. Weather this is specific to the investigated case or organism or a more general feature, cannot be deduced here, but will surely be an interesting question, when applying such approaches to other organisms.

5. Concluding remarks

The enormous progress in genome sequencing has provided a number of valuable tools for stoichiometric modeling and optimization of metabolic networks (Segre et al., 2002; Patil et al., 2005; Pharkya and Maranas, 2006; Suthers et al., 2007; Trinh et al., 2008; Park et al., 2010; Becker et al., 2011). These are attractive from their straightforward strategy to directly exploit stoichiometric network information and allow broad simulation studies on various aspects (Kim et al., 2008). So far, the integrated analysis of *in vivo* and *in silico* fluxes is still rare (Beurton-Aimar et al., 2011). The present work integrates physiological flux information from existing strains into strain design—by combining the power of the computational network simulation with the resolution of experimental network analysis on the flux level. Thus, it displays a straightforward and relevant extension of existing approaches. It will be interesting to apply it also to other microorganisms and see, if some general characteristics on metabolic networks can be elucidated. Beyond that it seems a straightforward tool to guide and accompany strain engineering and combine flux analysis *in vivo* and *in silico* at different stages of development. This might help narrow down the number of mutants to be potentially constructed—not only in recombinant protein production, but also in other production processes.

Acknowledgements

This work was financially supported within the framework of the Collaborative Research Center SFB 578 - from Gene to Product - by the German Research Foundation (DFG). The kind supply of the flux software FiatFLUX 1.67 by Nicola Zamboni is acknowledged.

Appendix A. Supplementary material

Supplementary data associated with this article can be found in the online version at doi:10.1016/j.ymben.2011.11.002.

References

Andersen, M.R., Nielsen, M.L., Nielsen, J., 2008. Metabolic model integration of the bibliome, genome, metabolome and reactome of *Aspergillus niger*. Mol. Syst. Biol. 4, 178.

Beurton-Aimar, M., Beauvoit, B., Monier, A., Vallee, F., Dieuaide-Noubhani, M., Colombie, S., 2011. Comparison between elementary flux modes analysis and 13C-metabolic fluxes measured in bacterial and plant cells. BMC Syst. Biol. 5, 95.

Becker, J., Klopprogge, C., Wittmann, C., 2008. Metabolic responses to pyruvate kinase deletion in lysine producing *Corynebacterium glutamicum*. Microb. Cell Fact. 7, 8.

Becker, J., Zelder, O., Häfner, S., Schröder, H., Wittmann, C., 2011. From zero to hero-design-based systems metabolic engineering of *Corynebacterium glutamicum* for l-lysine production. Metab. Eng. 13, 159–168.

Blank, L.M., Lehmbeck, F., Sauer, U., 2005. Metabolic-flux and network analysis in fourteen hemiascomycetous yeasts. FEMS Yeast Res. 5, 545–558.

Blank, L.M., Sauer, U., 2004. TCA cycle activity in *Saccharomyces cerevisiae* is a function of the environmentally determined specific growth and glucose uptake rates. Microbiology 150, 1085–1093.

David, H., Akesson, M., Nielsen, J., 2003. Reconstruction of the central carbon metabolism of *Aspergillus niger*. Eur. J. Biochem. 270, 4243–4253.

de Jongh, W.A., Nielsen, J., 2008. Enhanced citrate production through gene insertion in *Aspergillus niger*. Metab. Eng. 10, 87–96.

Diano, A., Bekker-Jensen, S., Dynesen, J., Nielsen, J., 2006. Polyol synthesis in *Aspergillus niger*: influence of oxygen availability, carbon and nitrogen sources on the metabolism. Biotechnol. Bioeng. 94, 899–908.

Driouch, H., Hänsch, R., Wucherpfennig, T., Krull, R., Wittmann, C., 2011b. Improved enzyme production by superior bio-pellets of *Aspergillus niger*—targeted morphology engineering using titanate micro particles. Biotechnol. Bioeng.. doi:10.1002/bit.23313.

Driouch, H., Roth, A., Dersch, P., 2011a. Filamentous fungi in good shape: microparticles for tailor-made fungal morphology and enhanced enzyme production. Bioeng. Bugs 2, 1–5.

Driouch, H., Roth, A., Dersch, P., Wittmann, C., 2010a. Optimized bioprocess for production of fructofuranosidase by recombinant *Aspergillus niger*. Appl. Microbiol. Biotechnol. 87, 2011–2024.

Driouch, H., Sommer, B., Wittmann, C., 2010b. Morphology engineering of *Aspergillus niger* for improved enzyme production. Biotechnol. Bioeng. 105, 1058–1068.

Fiaux, J., Cakar, P.Z., Sonderegger, M., Wüthrich, K., Szyperski, T., Sauer, U., 2003. Metabolic-flux profiling of the yeasts *Saccharomyces cerevisiae* and *Pichia stipitis*. Eukaryotic Cell 2, 170–180.

Fleissner, A., Dersch, P., 2010. Expression and export: recombinant protein production systems for *Aspergillus*. Appl. Microbiol. Biotechnol. 87, 1255–1270.

Fredlund, E., Blank, L.M., Schnürer, J., Sauer, U., Passoth, V., 2004. Oxygen- and glucose-dependent regulation of central carbon metabolism in *Pichia anomala*. Appl. Env. Microbiol. 70, 5905–5911.

Hofmann, G., Diano, A., Nielsen, J., 2009. Recombinant bacterial hemoglobin alters metabolism of *Aspergillus niger*. Metab. Eng. 11, 8–12.

Jouhten, P., Pitkänen, E., Pakula, T., Saloheimo, M., Penttilä, M., Maaheimo, H., 2009. 13C-metabolic flux ratio and novel carbon path analyses confirmed that *Trichoderma reesei* uses primarily the respirative pathway also on the preferred carbon source glucose. BMC Syst. Biol. 3, 104.

Kiefer, P., Heinzle, E., Zelder, O., Wittmann, C., 2004. Comparative metabolic flux analysis of lysine-producing *Corynebacterium glutamicum* cultured on glucose or fructose. Appl. Environ. Microbiol. 70, 229–239.

Kim, H.U., Kim, T.Y., Lee, S.Y., 2008. Metabolic flux analysis and metabolic engineering of microorganisms. Mol. Biosyst. 2, 113–120.

Lubertozzi, D., Keasling, J.D., 2009. Developing *Aspergillus* as a host for heterologous expression. Biotechnol. Adv. 27, 53–75.

Maiorano, E.A., Piccoli, R.M., da Silva, E.S., Rodrigues, D.A.M.F., 2008. Microbial production of fructosyltransferases for synthesis of pre-biotics. Biotech. Lett. 30, 1867–1877.

Meijer, S., Otero, J., Olivares, R., Andersen, M.R., Olsson, L., Nielsen, J., 2009. Overexpression of isocitrate lyase-glyoxylate bypass influence on metabolism in *Aspergillus niger*. Metab. Eng. 11, 107–116.

Melzer, G., Esfandabadi, M.E., Franco-Lara, E., Wittmann, C., 2009. Flux design: in silico design of cell factories based on correlation of pathway fluxes to desired properties. BMC. Syst. Biol. 3, 120.

Nevalainen, H., Te'o, V., Penttilä, M.J., Pakula, T., 2005. Heterologous gene expression in filamentous fungi: a holistic view alert. Appl. Mycol. Biotechnol. 5, 211–237.

Nielsen, J., Villadsen, J., 1994. Bioreaction Engineering Principles, 2nd ed. Kluwer Plenum Publishers, ISBN: 0-306-47349-6.

Panagiotou, G., Andersen, M.R., Grotkjaer, T., Regueira, T.R., Nielsen, J., Olsson, L., 2009a. Studies of the production of fungal polyketides in *Aspergillus nidulans* using systems biology tools. Appl. Env. Microbiol. 75, 2212–2220.

Panagiotou, G., Grotkjaer, T., Hofmann, G., Bapat, P.M., Olsson, L., 2009b. Overexpression of a novel endogenous NADH kinase in Aspergillus nidulans enhances growth. Metab. Eng. 11, 31–39.

Park, J.M., Kim, T.Y., Lee, S.Y., 2010. Prediction of metabolic fluxes by incorporating genomic context and flux-converging pattern analyses. PNAS 107, 14931–14936.

Patil, K.R., Rocha, I., Forster, J., Nielsen, J., 2005. Evolutionary programming as a platform for in silico metabolic engineering. BMC Bioinform. 6, 308.

Pedersen, H., Carlsen, M., Nielsen, J., 1999. Identification of enzymes and quantification of metabolic fluxes in the wild type and in a recombinant *Aspergillus oryzae* strain. Appl. Env. Microbiol. 65, 11–19.

Pedersen, H., Christensen, B., Hjort, C., Nielsen, J., 2000. Construction and characterization of an oxalic acid nonproducing strain of *Aspergillus niger*. Metab. Eng. 41, 34–41.

Pharkya, P., Maranas, C.D., 2006. An optimization framework for identifying reaction activation/inhibition or elimination candidates for overproduction in microbial systems. Metab. Eng. 8, 1–13.

Pool-Zobel, B., van Loo, J., Rowland, I., Roberfroid, M.B., 2002. Experimental evidences on the potential of prebiotic fructans to reduce the risk of colon cancer. Br. J. Nutr. 87, 273–281.

Schmidt, K., Norregaard, L.C., Pedersen, B., Meissner, A., Duus, J., Nielsen, J., Villadsen, J., 1999. Quantification of intracellular metabolic fluxes from fractional enrichment and 13C-13C coupling constraints on the isotopomer distribution in labeled biomass components. Metab. Eng. 1, 166–179.

Segre, D., Vitkup, D., Church, G.M., 2002. Analysis of optimality in natural and perturbed metabolic networks. PNAS 99, 15112–15117.

Sola, A., Maaheimo, H., Ylönen, K.P.F.T.S., 2004. Amino acid biosynthesis and metabolic flux profiling of *Pichia pastoris*. Eur. J. Biochem. 271, 2462–2470.

Suthers, P.F., Burgard, A.P., Dasika, M.S., Nowroozi, F., Van Dien, S., Keasling, J.D., Maranas, C.D., 2007. Metabolic flux elucidation for large-scale models using 13C labeled isotopes. Metab. Eng. 9, 387–405.

Trinh, C.T., Unrean, P., Srienc, F., 2008. Minimal *Escherichia coli* cell for the most efficient production of ethanol from hexoses and pentoses. Appl. Environ. Microbiol. 74, 3634–3643.

Wittmann, C., 2007. Fluxome analysis using GC–MS. Microb. Cell Fact. 6, 6.

Wittmann, C., Hans, M., Heinzle, E., 2002. *In vivo* analysis of intracellular amino acid labelings by GC–MS. Anal. Biochem 307, 379–382.

Wittmann, C., Heinzle, E., 2002. Genealogy profiling through strain improvement using metabolic network analysis: metabolic flux genealogy of several generations of lysine-producing corynebacteria. Appl. Environ. Microbiol. 68, 5843–5859.

Zamboni, N., Fischer, E., Sauer, E., 2005. FiatFlux—a software for metabolic flux analysis from 13C-glucose experiments. BMC Bioinform. 6, 209.

Zuccaro, A., Götze, S., Kneip, S., Dersch, P., Seibel, J., 2008. Tailor-made fructooligosaccharides by a combination of substrate and genetic engineering. Chem. Bio. Chem. 9, 143–149.